Applying Model-Agnostic Meta-Learning with Iterative Dichotomiser 3 for Alternating-Switching Active Noise Control Systems

Xiaoyi Shen*, Dongyuan Shi†, Woon-Seng Gan‡ and Jun Yang*
* State Key Laboratory of Acoustics and Marine Information, Institute of Acoustics, Chinese Academy of Sciences.
E-mail:xiaoyi003@e.ntu.edu.sg, jyang@mail.ioa.ac.cn
† Center of Intelligent Acoustics and Immersive Communications, Northwestern Polytechnical University
E-mail: dongyuan.shi@nwpu.edu.cn
‡ Digital Signal Processing Lab, Nanyang Technological University.
Email: ewsgan@ntu.edu.sg

***Abstract*—The convergence speed of adaptive algorithms has a significant impact on the dynamic noise reduction of the active noise control (ANC) system. Compared to some conventional approaches (variable step size, etc.), model-agnostic meta-learning (MAML) initialization has been demonstrated to be a low-cost but highly efficient method for improving convergence speed. However, MAML only initiates the optimal weights one time and cannot account for environmental variation during the ANC process. Hence, this paper proposes an alternating switching mechanism (ASM) that re-initializes the control filter's weight when detecting acoustic variations. Furthermore, the iterative dichotomiser 3 (ID3) algorithm is utilized to determine the threshold of ASM for identifying environmental variation instead of trial and error. Numerical simulations demonstrate the effectiveness of the proposed method in a varying acoustic environment.**

***Index Terms*—Active noise control (ANC), model-agnostic meta-learning (MAML), alternating switching mechanism, ID3**

I. Introduction

Active noise control (ANC) systems are widely employed to attenuate various noises [1]–[7], which generates the anti-noise through the adaptive filter that maintains the same amplitude as the noise but with an opposite phase [8]–[11]. Getting the adaptive filter to converge quickly to the steady state is essential in real-world applications such as ANC headphones, headrests, and windows [12]–[15]. Numerous strategies have been employed to improve the convergence speed of the adaptive filter. Some modified adaptive algorithms have been proposed: Normalized filtered-X least mean square (NFXLMS) algorithm adjusts the step size based on the input power to control the convergence speed, and the recursive least square (RLS) [16], [17] iteratively updates the parameters of the adaptive filter to minimize errors between predicted and actual outputs. Furthermore, various techniques involving variable step sizes are employed in the ANC implementation [18], [19]. These adjustments in adaptive algorithms are designed to improve convergence speed, especially in situations characterized by dynamic environmental changes. However, the increased computational complexity that these algorithms introduce has limited their practical applications.

The initial weight of the control filter also plays an essential role in determining the convergence speed, as it determines the subsequent steps leading to the optimal control filter [20]. Most conventional ANC applications employ a random or zero initial weight, resulting in a long convergence time from the initial state to the steady state [21], [22]. To address this issue, optimization techniques have been proposed to determine the optimal initial weight of the adaptive filter, thereby reducing the required steps to reach the optimal weight. Particle swarm optimization (PSO) is proposed to initialize a group of particles and iteratively explore the search space to identify the optimal initial weight [23], [24]. However, PSO may converge to local optima, which potentially slows down the convergence speed of the adaptive algorithm. Alternatively, the model-agnostic meta-learning (MAML) approach has been applied to get the optimal initial weight [25]–[27]. MAML collects various disturbances and primary noises from diverse acoustic environments to derive the optimal initial weight, enabling the FXLMS algorithm to converge within a few steps. Furthermore, the offline training of the optimal initial weights using PSO and MAML reduces computational complexity.

However, the issue of slow convergence still exists when the acoustic environment changes, even if the optimal initial weight is utilized at the beginning stage of ANC. Resetting the optimal initial weight of the adaptive filter when environmental changes are detected can address this challenge. The main task of resetting is to detect environmental changes. Previously, a threshold value calculated by trial-and-error was applied to evaluate the reset timing [28], [29]. This paper proposes an improved method to automate the threshold-setting procedure through the Iterative Dichotomiser 3 (ID3) algorithm. The alternating switching mechanism (ASM), driven by the output of ID3, resets the control filter weight in response to the normalized mean square errors (NMSE) and the slope of the mean square error(Slope).

979-8-3315-7206-8/25/$31.00

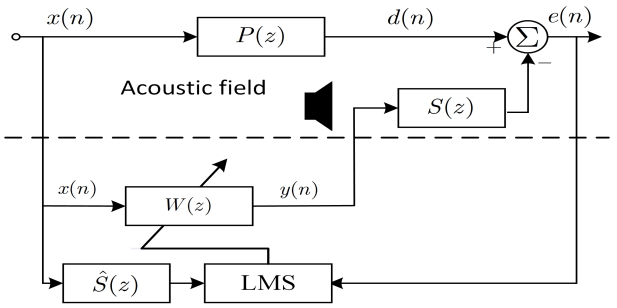

Fig. 1. The block diagram of feedforward ANC applying FXLMS algorithm.

II. Proposed method

This section proposes the MAML algorithm equipped with ASM (MAML-ASM) to attenuate the noise in a dynamic environment. Furthermore, an ID3 algorithm is employed to replace the manual selection of the threshold in ASM.

A. Feedforward ANC with adaptive algorithm

A feedforward structure is commonly employed to generate the control signal of ANC:

$$y(n) = \mathbf{x}(n)\mathbf{w}^{\mathrm{T}}(n), \tag{1}$$

where $\mathbf{x}(n) = [x(n), x(n-1), \cdots, x(n-L+1)]^{\mathrm{T}}$ and $\mathbf{w}(n) = [w_0(n), w_1(n), \cdots, w_{L-1}(n)]^{\mathrm{T}}$ denotes the reference signal picked up by the reference sensor and the weight of the adaptive filter $W(z)$, respectively. L represents the length of the control filter. Hence, the error signal $e(n)$ picked up by the error sensor is obtained from

$$e(n) = d(n) - y(n) * \mathbf{s}(n), \tag{2}$$

where $d(n)$ stands for the disturbance to be attenuated, and $*$ denotes the convolution operation. $\mathbf{s}(n)$ is the impulse response of the secondary path.

The weights of the control filter are updated by filtered-X least mean square (FXLMS) [21], [30]:

$$\mathbf{w}(n+1) = \mathbf{w}(n) - \mu\mathbf{x}'(n)e(n), \tag{3}$$

where μ is the step size in the FXLMS algorithm and $\mathbf{x}'(n)$ denotes the reference signal filtered by the estimated secondary path $\hat{\mathbf{s}}(n)$.

The weight error vector between $\mathbf{w}(n)$ and the optimal weight $\mathbf{w}^o$ can be derived as

$$\mathbb{E}\left[\mathbf{w}(n) - \mathbf{w}^o\right] = (1 - \mu\eta_n)^{n-1}\mathbb{E}\left[\mathbf{w}(0) - \mathbf{w}^o\right], \tag{4}$$

where $\mathbb{E}[\cdot]$ represents the expectation of the argument. $\mathbf{w}(0)$ is the initial weight of the control filter, and η_k denotes the kth $(k = 1, 2, \cdots, L)$ eigenvalue of the power spectrum of $\mathbf{x}'(n)$.

According to (4), it can be found that the smaller distance between $\mathbf{w}(0)$ and $\mathbf{w}^o$, the fewer steps are needed for $\mathbf{w}(n)$ to reach the optimal weight. Therefore, determining the optimal initial weight $\mathbf{w}^o(0)$ for ANC initialization is essential for improving convergence speed.

B. Model-agnostic meta-learning algorithm (MAML)

The MAML algorithm is applied to find out $\mathbf{w}^o(0)$ in a feedforward ANC system. The training process for MAML can be divided into two parts: within-task training and cross-task training. In the within-task training, the sample $\mathbf{d}^\dagger(k)$ and $\mathbf{x}^\dagger(k)$ are randomly sampled from the set of pre-measured disturbance tracks $\{\mathbf{d}_1(n), \mathbf{d}_2(n), \cdots\}$ and set of filter reference signals $\{\mathbf{x}'_1(n), \mathbf{x}'_2(n), \cdots\}$ under different configuration settings of ANC. If the jth track has been sampled, the training data pair is given by

$$\begin{cases} \mathbf{d}^\dagger(k) & = \mathbf{d}_j(n) \\ \mathbf{x}^\dagger(k-i) = & \begin{bmatrix} x'_j(n-i) & x'_j(n-i-1) & \cdots & \mathbf{0}_{1\times i} \end{bmatrix}^{\mathrm{T}} \end{cases}. \tag{5}$$

The recursive formula of the MAML initial control filter can be expressed as

$$\mathbf{\Phi}(n+1) = \mathbf{\Phi}(n) + \epsilon \sum_{i=0}^{N-1} \lambda^i e(k-i)\mathbf{x}^\dagger(k-i), \tag{6}$$

where $\lambda \in [0, 1]$ is the forgetting factor, and $\epsilon \in (0, 1)$ is the learning rate. The within-training error signal is represented as

$$e^\dagger(k-i) = d^\dagger(k-i) - \varphi^{\mathrm{T}}(n)\mathbf{x}^\dagger(k-i). \tag{7}$$

The control filter in (7) is updated by

$$\varphi(n) = \mathbf{\Phi}(n) - \mu e^\dagger(k)\mathbf{x}'(k), \tag{8}$$

In the cross-task training, the cross-task error signal is obtained from

$$e^\star(k) = d(k) - \mathbf{\Phi}^{\mathrm{T}}(n)\mathbf{x}'(k). \tag{9}$$

As (6) approaches convergence, we save $\mathbf{\Phi}(n)$ as the optimal initial weight $\mathbf{w}^o(0)$. $\mathbf{w}^o(0)$ is offline-trained and utilized to initialize the FXLMS algorithm, which will finally achieve the optimal control filter $\mathbf{w}^{\mathrm{o}}$ at the steady-state.

C. Alternating switching mechanism (ASM)

The FXLMS algorithm attempts to catch up with the changes in the acoustic environments, such as acoustic paths and primary noise variations. However, these changes tend to slow down the convergence of the FXLMS algorithm. In such instances, a practical approach to improve convergence speed is to reset the control filter to $\mathbf{w}^o(0)$, especially if the particular variation aligns with the training dataset used by the MAML algorithm.

Therefore, ASM is integrated into the adaptive process of ANC to reset the control filter. The detailed pseudocode illustrating the ASM, coupled with the ID3 algorithm, is provided in Table 1. In ASM, two factors are used to evaluate if the weight should be reset: the logarithm of the normalized mean square error (NMSE) and the slope of the MSE. The logarithm of NMSE is obtained from

$$\text{NMSE} = 10\log_{10}\{\sum_{i=0}^{N_m-1} e^2(n-i) / \sum_{i=0}^{N_m-1} e^2(i)\}, \tag{10}$$

where N_m is the average number. The slope of the MSE (Slope) is calculated by

$$S_p = \frac{1}{N_T} \sum_{i=0}^{N_T-1} e(n-i)\left[e(n-i) - e(n-i-1)\right], \quad (11)$$

where N_T denotes the number of average samples used to smooth the slope.

The values of NMSE and Slope increase to a large extent when the acoustic environment changes, causing a disruption in the convergence state. The challenge for ASM is to choose the threshold according to the NMSE and Slope in every iteration to decide whether to reset the control filter. Manual selection of threshold is not suitable in different situations, and in the following section, we provide a reliable method employing ID3 to decide the threshold.

D. Threshold determined by Iterative Dichotomiser 3 (ID3)

The ID3 algorithm [31], [32] is employed to assess the necessity of resetting the control filter's weight to $\mathbf{w}^o(0)$. The results of (10) and (11) during each iteration are inputted into the ID3 algorithm. Subsequently, the ID3 algorithm's output determines whether resetting is needed or not for ASM. M pairs of NMSE, Slope (reordered by the value), and Reset Flag are prepared in the training process of ID3. To simplify, we only mention NMSE in the following description.

The entropy of the Reset Flag in the dataset T_{NMSE} is calculated as follows:

$$H(\text{ResetFlag}) = -[P_r \log_2 P_r + (1-P_r)\log_2(1-P_r)], \quad (12)$$

where P_r is the probability of the Reset Flag in the dataset.

In order to deal with the continuous value of NMSE in the dataset T_{NMSE} ($T_{\text{NMSE}} = \text{NMSE}^1, \text{NMSE}^2, \cdots, \text{NMSE}^M$), midpoints between consecutive values of NMSE are calculated as potential split points:

$$T^m_{\text{NMSE}} = \{\frac{\text{NMSE}^m + \text{NMSE}^{m+1}}{2}\}, \quad (13)$$

where $m = 1, 2, \cdots, M$. The midpoints T^m_{NMSE} divide the NMSE dataset into two subsets:

$$\begin{cases} T^{m-}_{\text{NMSE}} = \{\text{NMSE}^1, \text{NMSE}^2, \cdots, \text{NMSE}^{m-1}\} \\ T^{m+}_{\text{NMSE}} = \{\text{NMSE}^m, \text{NMSE}^{m+1}, \cdots, \text{NMSE}^M\}. \end{cases} \quad (14)$$

The entropy of the midpoints can be calculated as

$$\begin{aligned} &H(T^{m+(-)}_{\text{NMSE}}) = \\ &-[P^{+(-)}\log_2 P^{+(-)} + (1-P^{+(-)})\log_2(1-P^{+(-)})], \end{aligned} \quad (15)$$

where $P^{+(-)}$ denotes the probability of the Reset Flag in the subset $T^{m+(-)}_{\text{NMSE}}$. The information gain of the midpoint is calculated as:

$$\begin{aligned} &Gain(\text{ResetFlag}, \text{NMSE}, m) = H(\text{ResetFlag}) - \\ &\frac{|D(T^{m-}_{\text{NMSE}})|}{|D(\text{ResetFlag})|} H(T^{m-}_{\text{NMSE}}) - \frac{|D(T^{m+}_{\text{NMSE}})|}{|D(\text{FesetFlag})|} H(T^{m+}_{\text{NMSE}}), \end{aligned} \quad (16)$$

Algorithm 1: Pseudo code of MAML-ASM with ID3 algorithm

Initializing:Optimal initial control filter $\mathbf{w}^o(0)$, step size μ,
while n **do**
  /* Control filter weight updating */
  $e(n) = d(n) - \mathbf{x}'^{\mathrm{T}}(n)\mathbf{w}(n)$.
  $\mathbf{w}(n+1) = \mathbf{w}(n) + \mu e(n)\mathbf{x}'(n)$.
  /* Flag setting by ID3 algorithm */
  Input: NMSE, S_p
  NMSE $= 10 * \log_{10}\{\sum_{i=0}^{N_m-1} e^2(n-i) / \sum_{i=0}^{N_m-1} e^2(i)\}$,
  $S_p = \frac{1}{N_T}\sum_{i=0}^{N_T-1} e(n-i)\left[e(n-i) - e(n-i-1)\right]$
  Output: Reset Flag
  /* ASM determination */
  if Reset Flag =1
  $\mathbf{w}(n+1) = \mathbf{w}^o(0)$
  $n \leftarrow n+1$.

where $|D(T^{m+(-)}_{\text{NMSE}})|$ denotes the number of instances (Reset Flag =1) in subset $T^{m+(-)}_{\text{NMSE}}$, and $|D(\text{ResetFlag})|$ denotes the number of instances (Reset Flag =1) in the dataset T_{NMSE}, and the optimal split point is chosen as:

$$Gain = \max_{m \in M} Gain(\text{ResetFlag}, \text{NMSE}, m), \quad (17)$$

in which the highest information gain is chosen as the threshold in ASM.

There are two scenarios in which ID3 makes a false decision: the first involves a static acoustic environment where the weight is reset, and in the second, the environment changes, but the ASM decides not to reset. In the first case, the weight is promptly reset to its initial value but rapidly converges to the optimal value. In the second case, the ANC system will converge to the new optimal value at a slower speed.

III. Simulation Results

Simulations are conducted to verify the efficacy of the ANC system, which employs $\mathbf{w}^o(0)$ trained through MAML and reset using ASM across various scenarios. In the training phase of optimal initial weight via MAML, a broadband noise (100−1500Hz) serves as the primary noise. The dataset comprises reference signals and disturbances from four different primary paths measured from four corners of the experiment room. Each disturbance was given an equal share of 25% of the total disturbances. This dataset is then divided, with 70% allocated for the training set and the remaining 30% for the testing set.

A. Threshold determination

The dataset used to construct the ID3 algorithm is collected from a varying acoustic environment (50%) and a static environment (50%). The varying environment consists of variations occurring in the primary path (16.7%), the secondary path (16.7%), and the primary noise (16.7%). The remaining data is

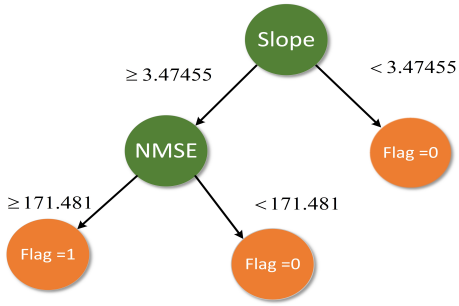

Fig. 2. The implementation of the ID3 algorithm with the threshold value for Slope = 3.47455 and NMSE = 171.481.

collected by ANC systems operating in a static environment. All data are partitioned, with 70% allocated to the training set and the remaining 30% to the test set.

Figure 2 illustrates the ID3 algorithm with an accuracy rate of 98.33% to decide the threshold for NMSE and Slope, while the false rate for misjudging the Reset Flag from 0 to 1 is 1.67%. The initial branch of the ID3 algorithm establishes the Slope and NMSE thresholds at 3.47455 and 171.481, respectively. If the Slope and NMSE surpass the thresholds, the Reset Flag is directly set to 1, prompting the control filter's weight to be reset to $\mathbf{w}^o(0)$. In cases where the NMSE is below 171.481, or the Slope is below 3.47455, the analysis progresses to the second branch, and the filter's weight remains unchanged.

B. Noise cancellation under accurate and false decisions

The simulation is taken to validate the noise reduction performance with the accurate and false decisions made by ID3. The primary noise is broadband noise with a frequency range of $300 - 800$ Hz; the length of the control filter and the sample rate are set to 1024 and 16 kHz, respectively. As a comparison, FXLMS with zero initialization (FXLMS), FXLMS with MAML initialization (MAML), and the proposed method (MAML-ASM) are carried out in the simulation.

Figure 3 (a) and (b) illustrate how MAML-ASM with ID3 algorithm performs in two different scenarios when making accurate decisions. Fig. 3 (a) demonstrates that when the acoustic environment is static (indicated by the Reset Flag remaining at 0), both MAML and MAML-ASM algorithms exhibit almost identical performance, surpassing the FXLMS algorithm with zero initialization. Fig. 3 (b) reveals that in a varying acoustic environment (where the Reset Flag is switched to 1), the MAML-ASM algorithm achieves the best noise reduction performance.

Furthermore, Fig. 3 (c) and (d) depict the noise reduction performance for MAML-ASM during false decisions in two different situations. Fig. 3 (c) shows a scenario where the Reset Flag is incorrectly set to 0 when detecting the changes in the acoustic environment. Consequently, the control filter's weight is not reset, leading to MAML and MAML-ASM having the same noise reduction performance. Fig. 3 (d) illustrates a case where the Reset Flag switches from 0 to 1 in a static

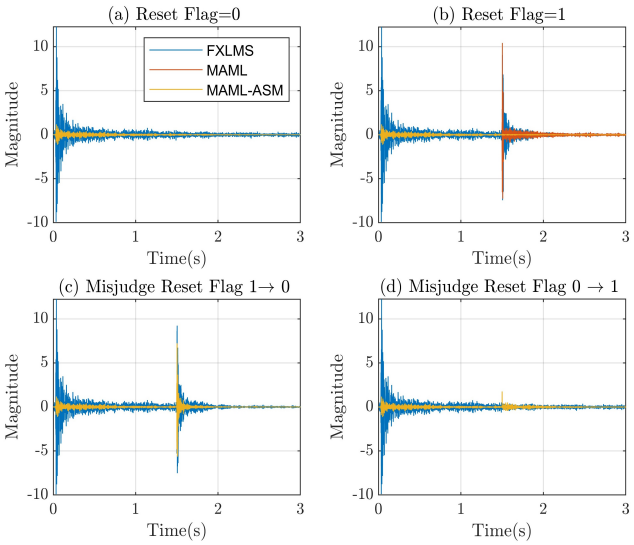

Fig. 3. The error signal of the algorithms when the resetting decision is accurate or false: (a) Accurate decision and Reset Flag =0; (b) Accurate decision and Reset Flag =1; (c) False decision and Reset Flag are misjudged from 1 to 0; (d) False decision and Reset Flag are misjudged from 0 to 1;

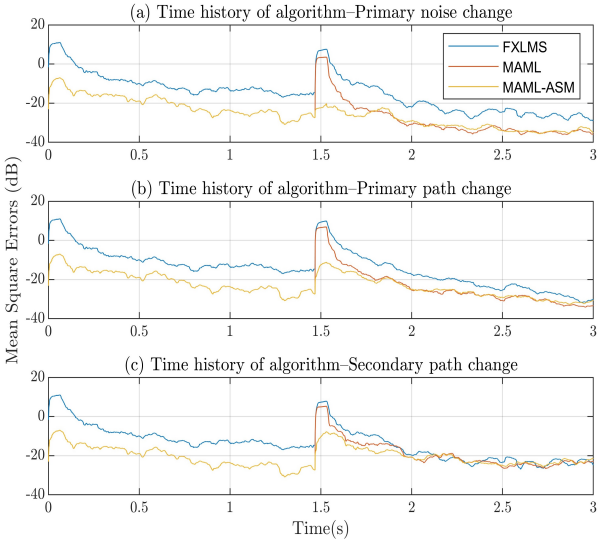

Fig. 4. The mean square errors and error signal of the algorithms in a varying acoustic environment: (a) primary noise change. (b) primary path change. (c) secondary path change.

environment. In this situation, MAML-ASM resets the weight and rapidly converges to the same status as MAML.

C. Noise cancellation for different varying environments.

This simulation tests the noise reduction performance when the acoustic environment undergoes changes. The simulation contains three different environmental variations: primary path change, secondary path change, and primary noise change (an uncorrelated noise occurring in the environment).

As seen in Fig. 4, MAML-ASM achieves the fastest convergence speed among the three varying environmental conditions, outperforming MAML and FXLMS. To illustrate how

MAML-ASM operates, the case of primary source changes is examined as an example. During the noise reduction process, a new uncorrelated primary noise (in the frequency range of $500 - 1000$Hz) emerges from the opposite direction of the initial primary noise. Consequently, the NMSE and Slope values experience a sudden increase, reaching values of 225.14 and 5.3032, respectively. Following the threshold set by the ID3 algorithm, the weight of the control filter is reset to $\mathbf{w}^o(0)$, which results in faster convergence of the adaptive algorithm.

IV. Conclusion

This paper demonstrated a novel method applied to an ANC system in dynamic acoustic environments. The proposed method integrated the model-agnostic meta-learning (MAML) algorithm to obtain the optimal initial weight and combined it with an alternating switching mechanism (ASM) to reset the control filter's weight in response to changing environments. Furthermore, the Iterative Dichotomiser 3 algorithm is utilized to eliminate the need for manual threshold selection to determine when to reset the optimal initial weight. Simulation results demonstrated that this proposed method achieved a faster convergence speed in adapting to changing acoustic conditions, surpassing conventional FXLMS techniques with random initial weights and outperforming MAML without the application of ASM.

Acknowledgment

This research is supported by the Chinese Academy of Sciences Talent Introduction Program for Young Researchers (Grant Number: 552025000180).

References

[1] S. M. Kuo and D. R. Morgan, *Active noise control systems*. Wiley, New York, 1996, vol. 4.

[2] S. J. Elliott and P. A. Nelson, "Active noise control," *IEEE signal processing magazine*, vol. 10, no. 4, pp. 12–35, 1993.

[3] C. N. Hansen, *Understanding active noise cancellation*. CRC Press, 1999.

[4] C.-Y. Chang, X.-W. Liu, S. M. Kuo, *et al.*, "Active noise control for centrifugal and axial fans," *Noise Control Engineering Journal*, vol. 68, no. 6, pp. 490–500, 2020.

[5] J. Cheer, S. J. Elliott, Y. Kim, and J.-W. Choi, "Practical implementation of personal audio in a mobile device," *Journal of the audio engineering society*, vol. 61, no. 5, pp. 290–300, May 2013.

[6] F. Yang, Y. Cao, M. Wu, F. Albu, and J. Yang, "Frequency-domain filtered-x lms algorithms for active noise control: A review and new insights," *Applied Sciences*, vol. 8, no. 11, p. 2313, 2018.

[7] H. Zhang and D. Wang, "Deep mcanc: A deep learning approach to multi-channel active noise control," *Neural Networks*, vol. 158, pp. 318–327, 2023.

[8] Y. Kajikawa, W.-S. Gan, and S. M. Kuo, "Recent advances on active noise control: Open issues and innovative applications," *APSIPA Transactions on Signal and Information Processing*, vol. 1, 2012.

[9] J. Chen, M. Wu, C. Gong, X. Wang, and J. Yang, "Steady-state performance analysis of the distributed fxlms algorithm for narrowband anc system with frequency mismatch," *IEEE Signal Processing Letters*, vol. 29, pp. 1167–1171, 2022.

[10] X. Shen, "Advanced active noise control headphone: Algorithm and implementation," 2023.

[11] W.-S. Gan, D. Shi, and X. Shen, "Practical active noise control: Restriction of maximum output power," *arXiv preprint arXiv:2307.10913*, 2023.

[12] D. Shi, W.-S. Gan, B. Lam, S. Wen, and X. Shen, "Optimal output-constrained active noise control based on inverse adaptive modeling leak factor estimate," *IEEE/ACM Transactions on Audio, Speech, and Language Processing*, vol. 29, pp. 1256–1269, 2021.

[13] H. Sun, T. D. Abhayapala, and P. N. Samarasinghe, "A realistic multiple circular array system for active noise control over 3d space," *IEEE/ACM Transactions on Audio, Speech, and Language Processing*, vol. 28, pp. 3041–3052, 2020.

[14] Y. Dong, J. Chen, and W. Zhang, "Wave-domain active noise control over distributed networks of multi-channel nodes," *Signal Processing*, vol. 184, p. 108 050, 2021.

[15] X. Shen, D. Shi, W.-S. Gan, and S. Peksi, "Adaptive-gain algorithm on the fixed filters applied for active noise control headphone," *Mechanical Systems and Signal Processing*, vol. 169, p. 108 641, 2022.

[16] Y. Xiao, L. Ma, K. Khorasani, A. Ikuta, and L. Xu, "A filtered-x rls based narrowband active noise control system in the presence of frequency mismatch," in *2005 IEEE International Symposium on Circuits and Systems (ISCAS)*, IEEE, 2005, pp. 260–263.

[17] N. Mohseni, T. W. Nguyen, S. A. U. Islam, I. V. Kolmanovsky, and D. S. Bernstein, "Active noise control for harmonic and broadband disturbances using rls-based model predictive control," in *2020 American Control Conference (ACC)*, IEEE, 2020, pp. 1393–1398.

[18] M. T. Akhtar, "A time-varying normalized step-size based generalized fractional moment adaptive algorithm and its application to anc of impulsive sources," *Applied Acoustics*, vol. 155, pp. 240–249, 2019.

[19] S. Ahmed and M. T. Akhtar, "Gain scheduling of auxiliary noise and variable step-size for online acoustic feedback cancellation in narrow-band active noise control systems," *IEEE/ACM Transactions on Audio, Speech, and Language Processing*, vol. 25, no. 2, pp. 333–343, 2016.

[20] X. Shen, D. Shi, Z. Luo, J. Ji, and W.-S. Gan, "A momentum two-gradient direction algorithm with variable step size applied to solve practical output constraint issue for active noise control," in *ICASSP 2023-2023*

IEEE International Conference on Acoustics, Speech and Signal Processing (ICASSP), IEEE, 2023, pp. 1–5.

[21] D. Shi, B. Lam, J. Ji, X. Shen, C. K. Lai, and W.-S. Gan, "Computation-efficient solution for fully-connected active noise control window: Analysis and implementation of multichannel adjoint least mean square algorithm," *Mechanical Systems and Signal Processing*, vol. 199, p. 110 444, 2023.

[22] W. Yang, F. Han, and G. Wang, "Robust active noise control: Minimum output variance approach with least mean lp-norm algorithm," *IEEE Transactions on Circuits and Systems II: Express Briefs*, pp. 1–1, 2023.

[23] J. Kennedy and R. Eberhart, "Particle swarm optimization," in *Proceedings of ICNN'95-international conference on neural networks*, IEEE, vol. 4, 1995, pp. 1942–1948.

[24] N. V. George and G. Panda, "A particle-swarm-optimization-based decentralized nonlinear active noise control system," *IEEE Transactions on Instrumentation and Measurement*, vol. 61, no. 12, pp. 3378–3386, 2012.

[25] C. Finn, P. Abbeel, and S. Levine, "Model-agnostic meta-learning for fast adaptation of deep networks," in *International conference on machine learning*, PMLR, 2017, pp. 1126–1135.

[26] L. Zintgraf, K. Shiarli, V. Kurin, K. Hofmann, and S. Whiteson, "Fast context adaptation via meta-learning," in *International Conference on Machine Learning*, PMLR, 2019, pp. 7693–7702.

[27] D. Shi, W.-s. Gan, X. Shen, Z. Luo, and J. Ji, "What is behind the meta-learning initialization of adaptive filter?—a naive method for accelerating convergence of adaptive multichannel active noise control," *Neural Networks*, p. 106 145, 2024.

[28] X. Shen, W.-S. Gan, and D. Shi, "Alternative switching hybrid anc," *Applied Acoustics*, vol. 173, p. 107 712, 2021, ISSN: 0003-682X. DOI: https://doi.org/10.1016/j.apacoust.2020.107712. [Online]. Available: https://www.sciencedirect.com/science/article/pii/S0003682X20308161.

[29] X. Shen, W.-S. Gan, and D. Shi, "Multi-channel wireless hybrid active noise control with fixed-adaptive control selection," *Journal of Sound and Vibration*, vol. 541, p. 117 300, 2022, ISSN: 0022-460X. DOI: https://doi.org/10.1016/j.jsv.2022.117300. [Online]. Available: https://www.sciencedirect.com/science/article/pii/S0022460X22004837.

[30] X. Qiu and C. H. Hansen, "A study of time-domain fxlms algorithms with control output constraint," *The Journal of the Acoustical Society of America*, vol. 109, no. 6, pp. 2815–2823, 2001.

[31] C. Jin, L. De-Lin, and M. Fen-Xiang, "An improved id3 decision tree algorithm," in *2009 4th international conference on computer science & Education*, IEEE, 2009, pp. 127–130.

[32] W. Peng, J. Chen, and H. Zhou, "An implementation of id3-decision tree learning algorithm," *From web. arch. usyd. edu. au/wpeng/DecisionTree2. pdf Retrieved date: May*, vol. 13, 2009.